

and, consequently,

$$\Delta f \approx \Delta \rho_{22} (1 - \nu_2/\nu_1).$$

Thus, for  $\nu_2 > \nu_1$ ,  $\Delta f < 0$  the distribution function has a dip whereas for  $\nu_2 < \nu_1$  it has a peak ( $\Delta f > 0$ ).

In the latter situation where  $\nu_2 \ll \nu_1$ , the width of the narrow peak in the distribution function can be  $M/k \ll G/k$ .

We shall now carry out the averaging in Eq. (12) over the distribution function (13). Under the conditions given above and for

$$4\eta d^2 |E_0|^2 / \hbar^2 \ll \gamma_{\perp}^2 \ll M^2$$

the absorption coefficient is

$$k_j = k_0 \left( \epsilon + \frac{\gamma_{\perp}^2}{M^2} \right), \quad k_0 = \frac{3}{2} \pi \lambda^2 \frac{\gamma n}{\pi^2 \hbar k u_0}, \quad (16)$$

where  $n$  is the concentration of normal atoms and  $k$  is the classical absorption coefficient. It follows from the above expression that the absorption coefficient decreases strongly. This weakening in the absorption coefficient (in the absence of saturation when  $dE_0 \ll \hbar\gamma$ ) is not surprising and it is associated with the presence of a dip in the distribution function. If  $\Delta \neq 0$ , we can expect bleaching of the gas and formation of a flux. In Ref. 4 we also demonstrated the special properties of absorption of radiation when allowance is made for the

radiation pressure.

We shall conclude by noting that these effects allow us to extend the use of coherent resonant light in control of the translational degrees of freedom of a gas. The deep narrow dip in the distribution function, induced by resonant light, may prove very useful in high-resolution spectroscopy.

<sup>1</sup>A. P. Kazantsev, *Usp. Fiz. Nauk* **124**, 113 (1978) [*Sov. Phys. Usp.* **21**, 58 (1978)].

<sup>2</sup>I. V. Krasnov and N. Ya. Shaparev, *Opt. Commun.* **27**, 239 (1978).

<sup>3</sup>I. V. Krasnov and N. Ya. Shaparev, *Zh. Eksp. Teor. Fiz.* **77**, 899 (1979) [*Sov. Phys. JETP* **50**, 453 (1979)].

<sup>4</sup>I. V. Krasnov and N. Ya. Shaparev, *Pis'ma Zh. Tekh. Fiz.* **1**, 875 (1975) [*Sov. Tech. Phys. Lett.* **1**, 381 (1975)].

<sup>5</sup>F. Kh. Gel'mukhanov and A. M. Shalagin, *Pis'ma Zh. Eksp. Teor. Fiz.* **29**, 773 (1979) [*JETP Lett.* **29**, 711 (1979)].

<sup>6</sup>A. L. Kalyazin and V. N. Sazonov, *Kvantovaya Elektron.* (Moscow) **6**, 1620 (1979) [*Sov. J. Quantum Electron.* **9**, 956 (1979)].

<sup>7</sup>W. Lochte-Holtgreven (ed.), *Plasma Diagnostics*, American Elsevier, New York, 1968 (Russian transl., Mir, M., 1971).

Translated by A. Tybulewicz

## Photoionization of a hydrogenlike atom in a homogeneous electric field

V. D. Kondratovich and V. N. Ostrovskii

*Leningrad State University*

(Submitted 26 January 1980)

*Zh. Eksp. Teor. Fiz.* **79**, 395-408 (August 1980)

The dependence of the ionization cross section of a hydrogenlike atom in a constant homogeneous electric field on the frequency and on the polarization of the light wave is considered in a quasiclassical approximation. For light polarized parallel to the homogeneous field, the calculated cross section oscillates smoothly as a function of the light frequency at a photon energy close to the ionization potential of the atom, whereas in the case of perpendicular polarization there is practically no structure. The oscillations are not connected with above-barrier reflection or below-barrier resonances, but are due to the singularities of the electron motion in the final state. The oscillations are qualitatively interpreted in terms of the classical trajectories of the electron following the excitation. The positions of the minima of the structure agree with recently obtained experimental data.

PACS numbers: 32.80.Fb, 32.60.+i, 32.90.+a

### 1. INTRODUCTION

The study of the Stark effect on a hydrogenlike atom was one of the first problems of quantum mechanics<sup>1,2</sup> and has been the subject of many theoretical papers even in recent years (see, e.g., Refs. 3-5 and the bibliographies cited therein). Nonetheless, even certain qualitative aspects of the problem remain unclear. Thus, no theoretical investigation of the photoionization of an atom in a uniform electric field has been carried out to this day, and the oscillatory structure of the fre-

quency dependence of this process was observed in experiment only recently.<sup>6,7</sup> Much interest is paid in general of late to the study of the Stark effect on highly excited states, in view of the use of this effect for the study of Rydberg atoms, as well as of in view of the interesting fundamental features of this phenomenon (see, e.g., Ref. 8).

It is known that in the presence of a time-constant uniform electric field of intensity  $\mathcal{E}$  the energy spectrum of the atom becomes continuous and extends over

the entire energy axis from  $-\infty$  to  $+\infty$ . The internal region of the atom is surrounded by a three-dimensional potential barrier, whose minimum in the case of a Coulomb field of the atomic core corresponds to an energy  $E_c = -2\mathcal{E}^{1/2}$  ( $E=0$ ) corresponds to the ionization threshold in the absence of the field  $\mathcal{E}$ ; unless otherwise indicated, atomic units are used throughout). In the vicinity of this energy value and below, the quantization of the motion in the internal region of the potential well leads to the appearance of the previously indicated<sup>1-5</sup> quasistationary states, which go over as  $\mathcal{E} \rightarrow 0$  into the stationary states of the atom. In photoionization of the atom in a uniform electric field from some deeply lying level with energy  $E_0 < E_c$ , which is not strongly perturbed by the field, the quasistationary states should manifest themselves in the form of resonances.

Cross-section singularities of another type were first noted in Ref. 7 at positive and negative finite electron energy in the vicinity of the value  $E=0$  above the classical barrier, i.e., at  $E \geq E_c$ . The structure takes the form of smooth oscillations that modulate the cross section, and the structure is present if the vector of the electric field of the light wave is parallel to the vector of the uniform field intensity ( $\sigma$  polarization) and vanishes in the case of perpendicular polarization ( $\pi$  polarization). The depth of modulation of the cross section increases with increasing homogeneous field (this corresponds to a decrease of  $E_c < 0$ ), so that these oscillations cannot be caused by above-barrier reflections from the existing potential barrier, which are characterized by a decrease of the relative amplitude with increasing distance from the top of the potential barrier  $E_c$ . The existence of a structure above the ionization barrier must therefore be regarded as a principally new effect.

To interpret the effect, the authors of Ref. 7 have carried out numerical calculations of certain classical trajectories of an electron moving in a superposition of a Coulomb and homogeneous field. Among the trajectories were such that corresponded prior to ionization to multiple oscillations of the electron along the field direction. On this basis, to describe the structure of the cross section, a quantization condition was postulated for the effective one-dimensional potential; this condition describes well the positions of the cross-section maxima observed in the experiment. Such a one-dimensional model is quite crude, as is seen from the fact that different authors<sup>7,9</sup> formulate different effective quantization conditions and do not touch at all upon the questions of the shapes and widths of the maxima and the depth of the modulation of the cross section.

In the present paper we explain the effect by starting from the singularities of the motion of the electron in the final state, where the constant field must be taken into account together with the atomic field. The influence of the field on the initial state can be neglected, and the alternating field of the light wave is taken into account by perturbation theory in the dipole approximation. The electron-trajectory singularities corresponding to the confined character of the motion along

one of the parabolic coordinates leads to the fact that an electron excited by a  $\pi$ -polarized light wave spends some time near the atomic core before it goes off to infinity. In the case of  $\sigma$  polarization of the light wave, the excited electron leaves the atom perpendicular to the homogeneous field and the delay effect is much less. The noted singularities of the classical motion manifest themselves in a quantum analysis in the quantization of the motion along one of the parabolic coordinates and in the substantial dependence of the partial photoionization cross sections on the polarization of the light. The paper contains a quantitative theory of the effect for a hydrogenlike atom (Sec. 2), based on a quasiclassical approximation (Sec. 3), as well as its interpretation from the point of view of classical three-dimensional trajectories of the electron in the considered system (Sec. 4) and a comparison with experiment (Sec. 5).

## 2. PHOTOIONIZATION CROSS SECTION IN THE PRESENCE OF A UNIFORM FIELD

It is common knowledge<sup>1,2</sup> that for a hydrogen atom placed in a homogeneous electric field directed along the  $z$  axis, upon separation of the variables in the parabolic coordinates  $\xi = r + z$ ,  $\eta = r - z$ ,  $\varphi = \arctg(y/x)$  the eigenfunction is sought in the form

$$\psi = (2\pi\xi\eta)^{1/2} \chi_1(\xi) \chi_2(\eta) e^{im\varphi}, \quad (2.1)$$

where the functions  $\chi_1(\xi)$ ,  $\chi_2(\eta)$  satisfy the equations

$$-\frac{d^2\chi_1}{d\xi^2} + \left[ \frac{E}{2} + \frac{Z_1}{\xi} - \frac{m^2-1}{4\xi^2} - \frac{1}{4}\mathcal{E}\xi \right] \chi_1 = 0, \quad (2.2)$$

$$-\frac{d^2\chi_2}{d\eta^2} + \left[ \frac{E}{2} + \frac{Z_2}{\eta} - \frac{m^2-1}{4\eta^2} + \frac{1}{4}\mathcal{E}\eta \right] \chi_2 = 0, \quad (2.3)$$

$\xi, \eta \geq 0$ ;  $m$  is magnetic quantum number,  $Z_1$  and  $Z_2$  are the separation constants, and  $Z_1 + Z_2 = 1$ .

In accord with (2.2), motion along the coordinate  $\xi$  is always finite, and this specifies a connection, in the form of a quantization condition, between  $Z_1$  and  $E$ . Thus, in the quasiclassical approximation this condition takes the form

$$\int_{\xi'}^{\xi''} p_\xi d\xi = (N + 1/2)\pi, \quad (2.4)$$

where  $\xi'$  and  $\xi''$  are the turning points that limit the classical motion along  $\xi$ ,  $N$  is an integer, and

$$p_\xi = \left[ \frac{E}{2} + \frac{Z_1}{\xi} - \frac{m^2}{4\xi^2} - \frac{1}{4}\mathcal{E}\xi \right]^{1/2},$$

$$p_\eta = \left[ \frac{E}{2} + \frac{Z_2}{\eta} - \frac{m^2}{4\eta^2} + \frac{1}{4}\mathcal{E}\eta \right]^{1/2}.$$

It is customary<sup>3,5</sup> in the quasiclassical approximation to use for simplicity the approximate equality

$$\int_{\xi'}^{\xi''} p_\xi d\xi \approx \int_{\xi_0}^{\xi_1} \bar{p}_\xi d\xi + |m|\pi/2,$$

where  $\bar{p}_\xi$  differs from  $p_\xi$  in the absence of the centrifugal term  $m^2/4\xi^2$ ,  $\xi_0$  and  $\xi_1$  are points that limit the region of classical motion with respect to  $\xi$  with momentum  $p_\xi$ . Taking this into account, the quasiclassical quantization condition takes the form

$$\int_{\xi_0}^{\xi_1} \bar{p}_\xi d\xi = [n_\xi + 1/2 + (|m|+1)\pi], \quad (2.5)$$

where  $\eta_l = N - (|m| + 1)$  takes on the values 0, 1, 2, . . .

At any energy  $E$ , thus, we can determine  $Z_1$  and consequently  $Z_2 = 1 - Z_1$ . The determination of the wave function  $\psi$  is completed by integrating the equation for  $\chi_2$ , which always has a solution, since the effective potential contained in it decreases without limit as  $\eta \rightarrow \infty$ .

Thus, the wave function of the electron is characterized by three quantum numbers: the integers  $\eta_l$  and  $m$ , and the continuous  $E$ , corresponding to the presence of three known integrals of motion in the considered problem.<sup>10</sup> The eigenstates of the energy and of the projection of the angular momentum on the  $z$  axis are degenerate in the quantum number  $n_l$ . It will be shown below that it is precisely the discreteness of the  $n_l$  spectrum, due to the finite character of the motion along the coordinate  $\xi$ , which leads to the existence of oscillations of the photoionization in the region of near-zero energies.

The photoionization cross section takes in the dipole approximation the form

$$\sigma(E) = \frac{(2\pi)^2}{c} \sum_m \sum_{n_l} \sigma_{n_l m E}, \quad (2.6)$$

where  $c$  is the speed of light in vacuum,  $n_l$ ,  $m$ , and  $E$  are the quantum numbers of the final states of the electron  $\psi_{n_l m E}$ , normalized to  $\delta_{n_l n_l} \delta_{m m} \delta(E - E')$ ;  $\sigma_{n_l m E}$  is the partial cross section

$$\sigma_{n_l m E} = |\langle \Phi | \mathbf{e} | \psi_{n_l m E} \rangle|^2. \quad (2.7)$$

Here  $\mathbf{e}$  is the light-wave polarization vector and  $\Phi$  is the wave function of the initial state of the active electron in the atom.

The practically attainable intensities of the homogeneous external electric field are much lower than the intensities of the intra-atomic fields, i. e., the estimate  $|E| \gg \mathcal{E}$  is valid, where  $E_0 = -\alpha^2/2$  is the energy of the initial state of the electron. This allows us to neglect the potential of the homogeneous field in the localization region of the active electron of the atom in the initial state ( $r \leq 1/\alpha$ ), which in fact determines the partial cross section (2.7) in view of the rapid decrease of  $\Phi$  when  $r > 1/\alpha$ . In the region  $r \leq 1/\alpha$  the exact wave function  $\psi_{n_l m E}$  differs from the Coulomb function in the absence of a field only by a constant factor, as well as by the choice of the separation constants  $Z_1$  and  $Z_2$ ; for this Coulomb function we have in parabolic coordinates

$$\chi_1^k(\xi) = A_1(k\xi)^{(m+1)/2} \exp\left(-\frac{i}{2}k\xi\right) F\left(i\frac{Z_1}{k} + m + 1, m + 1; ik\xi\right), \quad (2.8)$$

$$\chi_2^k(\eta) = A_2(k\eta)^{(m+1)/2} \exp\left(-\frac{i}{2}k\eta\right) F\left(i\frac{Z_2}{k} + m + 1, m + 1; ik\eta\right), \quad (2.9)$$

where  $A_1$  and  $A_2$  are normalization constants that depend on  $n_l, m, E$ ;  $F(a, c, z)$  is a confluent hypergeometric function, and  $k = (2E)^{1/2}$ .

Considering the initial  $s$  state, we put  $\Phi = \pi^{-1/2} \alpha^{3/2} e^{-\alpha r}$ , after which the integrals in (2.7) can be calculated analytically. Simplifying the results with the aid of the relation  $|E/E_0|^{1/2} \ll 1$ , we obtain, depending on the po-

larization of the light wave, the following nonzero partial cross sections.

1)  $\pi$  polarization ( $\mathbf{e} \parallel \mathcal{E}$ ), only the final states with  $m = 0$  are populated:

$$\sigma_{n_l 0 E} = C^2 k^2 [Z_1(n_l) - Z_2(n_l)]^2 A_1^2 A_2^2. \quad (2.10)$$

2)  $\sigma$  polarization ( $\mathbf{e} \perp \mathcal{E}$ ), in the final states  $m = 1$ .

Recognizing that  $\sigma_{n_l 1 E} = \sigma_{n_l -1 E}$ , we consider for the sake of argument  $\sigma_{n_l 1 E}$ :

$$\sigma_{n_l 1 E} = C^2 k^2 A_1^2 A_2^2; \quad (2.11)$$

$$C = 16\pi^{-1/2} \alpha^{-1/2} (\alpha^{-1/2}) e^{-2/\alpha}. \quad (2.12)$$

If the wave function of the initial state contains a pre-exponential factor in the form of a polynomial, then we must substitute in (2.10) and (2.11) another value of  $C$ , obtained from (2.12) by suitable differentiation with respect to the parameter. To introduce into the calculations the Hartree-Fock wave functions, it is convenient to use their approximate analytic representation in terms of a sum of Slater orbitals.<sup>11</sup>

Thus, in the approximation assumed for the wave functions of the final state the dependence of the partial cross sections on the electric field is contained only in the product of the normalization constants  $A_1$  and  $A_2$  (and also in the factor  $Z_1(\eta_l) - Z_2(\eta_l)$  in (2.10)). The latter quantities are calculated in the quasiclassical approximation in Sec. 3

### 3. QUASICLASSICAL APPROXIMATION

Drukarev<sup>5</sup> has noted that the quasiclassical condition of quantization of the motion with respect to coordinate (2.5) is expressed in terms of the hypergeometric function  $F(a, b; z)$ , so that the connection between  $Z_1$  and  $E$  is obtained in a convenient parametric form.

At  $E < 0$  we have<sup>5</sup>

$$Z_1(n_l) = \frac{t}{4(1-t)^2} \frac{|k|^4}{\mathcal{E}}, \quad (3.1)$$

$$\frac{t}{(1-t)^{3/2}} F\left(-\frac{1}{2}, \frac{1}{2}, 2; -t\right) = 4 \left[ n_l + \frac{1}{2}(|m| + 1) \right] \frac{\mathcal{E}}{|k|^3}, \quad (3.2)$$

where the parameter  $t$  lies in the interval  $0 < t < 1$ .

At  $E > 0$  we consider two cases:

if  $k^3 < 3\pi[n_l + \frac{1}{2}(|m| + 1)]\mathcal{E}$ , then  $Z_1 > 0$  in the parameter  $t > 1$ :

$$Z_1(n_l) = \frac{t}{4(t-1)^2} \frac{k^4}{\mathcal{E}}, \quad (3.3)$$

$$\frac{t}{(t-1)^{3/2}} F\left(-\frac{1}{2}, \frac{1}{2}, 2; -t\right) = 4 \left[ n_l + \frac{1}{2}(|m| + 1) \right] \frac{\mathcal{E}}{k^3}; \quad (3.4)$$

if  $k^3 > 3\pi[n_l + \frac{1}{2}(|m| + 1)]\mathcal{E}$ , then  $Z_1 < 0$  and the parameter  $t > 1$ :

$$Z_1(n_l) = -\frac{t}{4(t+1)^2} \frac{k^4}{\mathcal{E}}, \quad (3.5)$$

$$\frac{(t-1)^2}{(t+1)^{3/2}} F\left(\frac{1}{2}, \frac{3}{2}, 3; 1-t\right) = 16 \left[ n_l + \frac{1}{2}(|m| + 1) \right] \frac{\mathcal{E}}{k^3}. \quad (3.6)$$

As follows from (3.5),  $Z_1$  is bounded:  $Z_1 \geq -E^{1/2}/4\mathcal{E}$  at  $E > 0$ .

Proceeding now to the determination of the normalization factors  $A_1$  and  $A_2$ , we note that the wave function

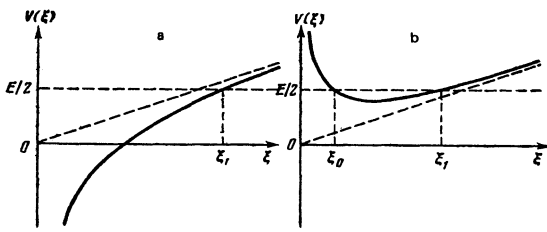


FIG. 1. Effective potential  $V(\xi)$  in Eq. (2.2) for  $\chi_1(\xi)$  at  $|m|=1$ ;  $\xi_0, \xi_1$ —turning points; a— $Z_1 > 0$ , b— $Z_1 < 0$  ( $\xi_0=0$  in case a).

(2.1) is already normalized to  $\delta_{mm}$ . An analysis of the normalization condition in parabolic coordinates shows that the functions  $\chi_1(\xi)$  and  $\chi_2(\xi)$  should be normalized in the following manner:

$$\int_0^\infty d\xi \frac{1}{\xi} \chi_{i, n_1, E}(\xi) \chi_{i, n_1, E'}(\xi) = 2\delta_{n_1 n_1'}, \quad (3.7)$$

$$\int_0^\infty d\eta \chi_{2, n_1, E}(\eta) \chi_{2, n_1, E'}(\eta) = 2\delta(E - E'). \quad (3.8)$$

We consider separately the cases  $m=0$  and  $m=1$  at  $E > 0$ . We begin with the simpler case  $m=1$ .

A plot of the effective potential  $V(\xi)$  in Eq. (2.2) where  $\chi_1(\xi)$  at  $m=1$  is shown in Fig. 1. To determine the quantity of  $A_1$  in the expression (2.8), we join together the quasiclassical function

$$\chi_1^{(k)}(\xi) = N_1 p_1^{-1/2} \cos\left(\int_{\xi_0}^{\xi} p_1 d\xi' + \frac{\pi}{4}\right) \quad (\xi < \xi_1) \quad (3.9)$$

which decreases exponentially at  $\xi > \xi_1$ , with the asymptotic form of the function (2.8). Depending on the ratio  $Z_1/k$ , the motion along the coordinate  $\xi$  is quasiclassical in different regions of variation of  $\xi$ . We use therefore the following asymptotic forms of the function (2.8):

a) at  $|Z_1|/k \geq 1$  for  $\xi \geq 1/Z_1$  in the region where the Coulomb field predominates

$$\chi_1^{(k)}(\xi) \approx \frac{A_1 k \xi^{3/2}}{\pi^{1/2} Z_1^{3/2}} \cos\left[2(Z_1 \xi)^{3/2} - \frac{3\pi}{4}\right]; \quad (3.10)$$

b) at  $|Z_1|/k \ll 1$  in the region where the Coulomb potential is much less than the energy  $E$

$$\chi_1^{(k)}(\xi) \approx 2A_1 \exp\left(-\frac{\pi Z_1}{2k}\right) \left(\frac{\pi Z_1}{k \operatorname{sh}(\pi Z_1/k)}\right)^{1/2} \cos\left(\int_{\xi_0}^{\xi} p_1 d\xi' - \frac{3\pi}{4}\right). \quad (3.11)$$

At  $|Z_1|/k \ll 1$  we obtain as a result of joining together in the last region

$$A_1 = \frac{N_1}{2k} \exp\left(\frac{\pi Z_1}{2k}\right) \left(\frac{\pi Z_1}{k \operatorname{sh}(\pi Z_1/k)}\right)^{1/2}. \quad (3.12)$$

The value of  $N_1$  is obtained by normalizing the quasiclassical function (3.9) in accordance with (3.7) using the customary scheme<sup>7</sup>:

$$N_1 = 2 \left(\int_{\xi_0}^{\xi_1} \frac{d\xi'}{\xi' p_1'}\right)^{-1/2} = \begin{cases} (2k/\pi)^{1/2} (t-1)^{-1/2} F(1/2, 1/2, 1; -t)^{-1/2} & \text{for } Z_1 > 0 \\ (2k/\pi)^{1/2} (1-t)^{-1/2} F(1/2, 1/2, 1; 1+t)^{-1/2} & \text{for } Z_1 < 0 \end{cases} \quad (3.13)$$

where

$$t = \frac{(1+16Z_1 \mathcal{E}/k^4)^{1/2} + 1}{(1+16Z_1 \mathcal{E}/k^4)^{1/2} - 1}. \quad (3.14)$$

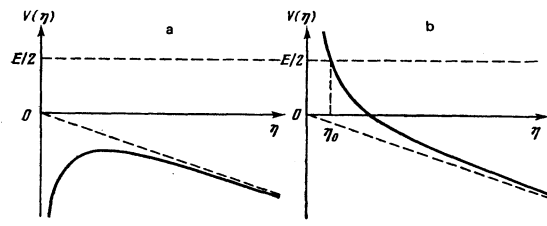


FIG. 2. Effective potential  $V(\eta)$  in Eq. (2.3) for  $\chi_2(\eta)$  at  $|m|=1$ ,  $\eta_0$ —turning point. a— $Z_2 > 0$ , b— $Z_2 < 0$ .

At  $Z_1/k \geq 1$  the matching is carried out in the region where the Coulomb potential predominates. Expression (3.13) is valid also in this case, and the expression for  $A_1$  coincides with the principal term of (3.12) at  $Z_1/k \gg 1$ .

A plot of the effective potential  $V(\eta)$  in Eq. (2.3) for  $\chi_2(\eta)$  at  $m=1$  is shown in Fig. 2. To determine  $A_2$  we join together the asymptotic form of the Coulomb function (2.9) with the quasiclassical wave function, whose normalization to  $2\delta(E - E')$  is determined by the asymptotic form as  $\eta \rightarrow \infty$ , where the homogeneous electric field predominates.

It is convenient in practice to compare the asymptotic form of the quasiclassical function with the asymptotic solution of the Airy equation, which describes the motion of the particle in a homogeneous field.<sup>1</sup> When normalized to  $2\delta(E - E')$ , the latter asymptotic form becomes

$$\chi_2^{(k)}(\eta) \approx \frac{2^{1/4}}{\pi^{1/2} \mathcal{E}^{1/4} x^{1/4}} \cos\left(\frac{2x^{3/2}}{3} + \delta\right), \quad (3.15)$$

where  $x = (\eta + k^2/\mathcal{E})(\mathcal{E}/4)^{1/3}$  and  $\delta$  is a certain phase. Continuation of the solution from the region where the Coulomb potential predominates with the aid of a quasiclassical function is effected in different ways, depending on the location of the zeros  $p_\eta$  in the complex  $\eta$  plane. The real parts of the roots  $p_\eta$  at  $|m|=1$  are opposite in sign to the energy  $E$ . This means that in the simplest quasiclassical approximation there is no reflection from the barrier.

When joining the values together we use the asymptotic representations for  $\chi_2^{(k)}(\eta)$ , similar to (3.10) and (3.11) for  $\chi_1^{(k)}(\xi)$ . At  $|Z_2|/k \ll 1$ , the joining of  $\chi_2^{(k)}(\eta)$  with the quasiclassical function is effected in the region of the maximum of  $V(\eta)$ , where  $p_\eta \approx k/2$ , and at  $Z_2/k \geq 1$  the joining is effected in the region where the Coulomb potential predominates. Comparing next the quasiclassical function with (3.15) as  $\eta \rightarrow \infty$ , we arrive at the following values:

at  $|Z_2|/k \ll 1$

$$A_2 = \frac{\exp(\pi Z_2/2k)}{2^{3/2} k} \left(\frac{Z_2}{\operatorname{sh}(\pi Z_2/k)}\right)^{1/2}; \quad (3.16)$$

at  $Z_2/k \geq 1$

$$A_2 = Z_2^{3/2} / 2^{1/2} k. \quad (3.17)$$

Since (3.17) is the principal term of (3.16) at  $Z_2/k \gg 1$ , it is natural to use (3.16) in the entire region  $Z_2/k \geq -1$ .

Thus, expressions (3.12) and (3.16), which are valid

in two limiting cases, can be regarded as interpolation formulas applicable respectively at all values  $Z_1/k \geq -1$  and  $Z_2/k \geq -1$ . We note that  $0 < E \ll 1$ , i. e.,  $k \ll 1$  in the considered energy region.

At  $Z_2/k \leq -1$ , the band where the Coulomb potential predominates is in a classically inaccessible region. Using in this region the asymptotic form

$$\chi_2^k(\eta) \approx \frac{A_2 k \eta^{1/2}}{2\pi^{1/2} |Z_1|^{1/2}} \exp(2|Z_1 \eta|^{1/2}), \quad (3.18)$$

we arrive at

$$A_2 = \frac{|Z_1|^{1/2}}{2^{1/2} k} \exp \left[ -\frac{\pi |Z_2|}{k} (1-x)^{1/2} F \left( -\frac{1}{2}, \frac{1}{2}, 2; -x \right) \right], \quad (3.19)$$

where

$$x = \frac{(1-16Z_2 \mathcal{E}/k^2)^{1/2} - 1}{(1-16Z_2 \mathcal{E}/k^2)^{1/2} + 1}. \quad (3.20)$$

Expressions (3.19) and (3.16) are joined together in the intermediate region of values of the ratio  $Z_2/k$ .

It is possible to modify analogously the expressions for  $A_1$  at  $Z_1/k \leq -1$ , but this is not necessary for the calculation for the cross section: the quantities  $A_1$  and  $A_2$  are exponentially small respectively at  $Z_1/k \leq -1$  and  $Z_2/k \leq -1$ , and the error due to the use of (3.12) and (3.16) in the entire region of variation of the ratios  $Z_1/k$  and  $Z_2/k$  is negligible.

Thus, for the partial cross section we obtain in accordance with formula (2.11) at  $Z_1 < 0$

$$\sigma_{n_i \pm E} = \frac{C^2 k e^{\pi/k} Z_1 Z_2}{2^{1/2} (1-t)^{1/2} F(1/2, 1/2, 1; 1+t) \text{sh}(\pi Z_1/k) \text{sh}(\pi Z_2/k)}; \quad (3.21)$$

at  $Z_1 > 0$

$$\sigma_{n_i \pm E} = \frac{C^2 k e^{\pi/k} Z_1 Z_2}{2^{1/2} (1-t)^{1/2} F(1/2, 1/2, 1; -t) \text{ch}(\pi Z_1/k) \text{sh}(\pi Z_2/k)}. \quad (3.22)$$

At  $m=0$ , Eqs. (2.2) and (2.3) contain centrifugal terms corresponding to attraction:  $1/4\xi^2$  and  $1/4\eta^2$ . We assume that their presence is fully accounted for by using the asymptotic expressions for the functions (2.8) and (2.9). By a procedure similar to that used above, we obtain the partial cross section  $\sigma_{n_i 0E}$ :

at  $Z_1 < 0$

$$\sigma_{n_i 0E} = \frac{C^2 k e^{\pi/k} (Z_1 - Z_2)^2}{2^{1/2} (1-t)^{1/2} F(1/2, 1/2, 1; 1+t) \text{ch}(\pi Z_1/k) \text{ch}(\pi Z_2/k)}; \quad (3.23)$$

at  $Z_1 > 0$

$$\sigma_{n_i 0E} = \frac{C^2 k e^{\pi/k} (Z_1 - Z_2)^2}{2^{1/2} (1-t)^{1/2} F(1/2, 1/2, 1; -t) \text{ch}(\pi Z_1/k) \text{ch}(\pi Z_2/k)}. \quad (3.24)$$

In (3.21)–(3.24) the quantities  $Z_1$  and  $Z_2$  are determined from  $n_i$ ,  $m$ ,  $E$ , and in accordance with (2.3)–(2.6) with allowance for the relation  $Z_1 + Z_2 = 1$ .

#### 4. SINGULARITIES OF THE PHOTOIONIZATION CROSS SECTION

Expressions (3.21)–(3.24) contain exponential factors that cut off the partial cross section outside the interval  $-k \leq Z_1 \leq 1+k$  or else, taking into account the smallness of  $k$  in the considered energy region  $0 < E \ll 1$ , outside the interval  $0 \leq Z_1 \leq 1$ . There are several values of  $n_i$  for which  $Z_1(n_i)$  are contained in the indicated interval; thus, at  $\mathcal{E} \sim 10^3$  V/cm their number is approximately 25, and at  $\mathcal{E} \sim 10$  V/cm their number is

about 100. The partial cross sections with  $Z_1$  not lying in this interval describe a low-probability transition into states in which the excited electron is quite far from the atomic nucleus.

A plot of the partial cross section against  $Z_1$  at  $m=0$  is a double-hump curve having maxima as small  $Z_1 > 0$  and at  $Z_1 \leq 1$ , the second of which is much narrower and the cross section in which is larger than in the first. At  $Z_1 = 0.5$  the cross section has a minimum where it vanishes. On the contrary, the partial cross section at  $m=1$  has a maximum at  $Z_1 \approx 0.5$  and vanishes at  $Z_1 = 0$  and at  $Z_1 = 1$ .

Formally the difference between these curves is connected with the presence in  $\sigma_{n_i 0E}$  of the factor  $(Z_1 - Z_2)^2 / \cosh(\pi Z_1/k) \cosh(\pi Z_2/k)$  in place of  $Z_1 Z_2 / \sinh(\pi Z_1/k) \sinh(\pi Z_2/k)$  in  $\sigma_{n_i \pm E}$  and with the small quantity  $k$  ( $k \sim 10^{-2}$  a. u.). The following explanation can be proposed for this difference. The quantum number  $n_i$  corresponds to the classical integral of motion (Ref. 10, p. 192)

$$\beta = Z_1 - Z_2 = -\frac{z}{r} - p_\rho(z p_\rho - \rho p_z) - \frac{p_\varphi^2}{\rho^2} z - \frac{\mathcal{E} \rho^2}{2}, \quad (4.1)$$

where  $\rho$ ,  $\varphi$ , and  $z$  are cylindrical coordinates with the  $z$  axis;  $p_\rho$  and  $p_\varphi$  are the momenta corresponding to the coordinates  $\rho$  and  $\varphi$ . Near the attracting center, where the influence of the uniform electric field can be neglected,  $\beta$  coincides with the  $z$  component of the Runge-Lenz vector [see (10), p. 53]—the additional integral of motion for the orbit in the Coulomb field.

The equality  $Z_1 = Z_2 = \frac{1}{2}$  denoted according to (4.1) that the excited electron executes near the attracting center a motion which is in first-order approximation along a hyperbola whose axis is perpendicular to the  $z$  axis. The electron is brought into such a state mainly by a light wave polarized perpendicular to the  $z$  axis, i. e., perpendicular to the uniform electric field. A light wave polarized parallel to the uniform field causes the electron to move predominantly along the  $z$  axis, i. e., with  $Z_1 \neq Z_2$ , and cannot impart motion perpendicular to this axis, and it is this which generates the dip on the plot of  $\sigma_{n_i 0E}$  at  $Z_1 = \frac{1}{2}$ .

In other terms, the vanishing of  $\sigma_{n_i 0E}$  at  $Z_1 = Z_2$  is due to the assumed approximation (2.8)–(2.9) for the wave function of the final state, according to which at  $Z_1 = Z_2$  there is symmetry with respect to reflection in the  $z=0$  plane. In view of the fact that the initial state has the same symmetry, the dipole transition under the influence of the  $\pi$  polarized wave turns out to be forbidden. For the exact wave function of the final state this selection rule is approximate.

To explain the maximum of  $\sigma_{n_i 0E}$  at  $Z_1 \approx 1$  it is necessary to resort to the singularity of the trajectories of the classical motion in the considered field, a singularity corresponding to the factor  $(t-1)^{-1/2} F(\frac{1}{2}, \frac{1}{2}, 1; -t)$  in both matrix elements. We make use here of the results of Beletskii<sup>12,13</sup> (see also his review<sup>14</sup>), who investigated flat trajectories, i. e., with zero moment relative to the symmetry axis, of the motion of a satellite in a Newtonian gravitational field when the satellite is acted upon by a constant vector of jet acceleration. This

problem corresponds mathematically to that of classical motion in the field considered by us.

After separating the variables in parabolic coordinates, the parametric equations of the trajectory are written out explicitly in terms of elliptic Jacobi functions.<sup>12</sup> At positive energy, the ratio of the periods  $T_\xi$  and  $T_\eta$  of the Jacobi functions that determine the motion along the parabolic coordinates  $\xi$  and  $\eta$  is equal to:

$$\text{if } Z_2 < 0 \\ \frac{T_\xi}{T_\eta} = \frac{(E^2 - 4\mathcal{E}Z_2)^{1/4} F(1/2, 1/2, 1; t/(t+1))}{(E^2 + 4\mathcal{E}Z_2)^{1/4} F(1/2, 1/2, 1; 1/(x+1))}; \quad (4.2)$$

$$\text{if } Z_2 > 0 \text{ and } E > 2(\mathcal{E}Z_2)^{1/2} \\ \frac{T_\xi}{T_\eta} = \frac{(E + (E^2 - 4\mathcal{E}Z_2)^{1/2})^{1/4} F(1/2, 1/2, 1; t/(t+1))}{2^{1/4} (E^2 + 4\mathcal{E}Z_2)^{1/4} F(1/2, 1/2, 1; x+1)}; \quad (4.3)$$

$$\text{if } Z_2 > 0 \text{ and } E < 2(\mathcal{E}Z_2)^{1/2} \\ \frac{T_\xi}{T_\eta} = \frac{2^{1/4} (\mathcal{E}Z_2)^{1/4} F(1/2, 1/2, 1; t/(t+1))}{(E^2 + 4\mathcal{E}Z_2)^{1/4} F(1/2, 1/2, 1; w)}, \quad (4.4)$$

where  $t$  and  $x$  are given by relations (3.14) and (3.20), and

$$w = [2(Z_2\mathcal{E})^{1/2} - E]/4Z_2^{1/2}.$$

It follows from (4.2)–(4.4) that at the inequality  $T_\xi/T_\eta \ll 1$  is satisfied, corresponding to the “serpentine” trajectory on Fig. 3. The turning point  $\xi_1$  (see Fig. 1) corresponds on Fig. 3 to the parabola (in space—a paraboloid of revolution) that limits the permissible region of the classical motion.

The inequality (4.5) is equivalent to a set of two restrictions:  $E \ll 2\mathcal{E}^{1/2}$  and  $|Z_2| = |1 - Z_1| \ll 1$ . Thus, an electron excited into a state with  $Z_1 \approx 1$  and energy  $E \ll 2\mathcal{E}^{1/2}$ , will spend some time near the atomic core before it goes off to infinity. Its motion is then practically along the  $z$  axis, in agreement with the results of the numerical calculation of the trajectories in Ref. 7. If the strict equality  $Z_1 = 1$  holds, then as  $t \rightarrow -\infty$  (here  $t$  is the time) the trajectory approaches to oscillations along the  $z$  axis between the top of the boundary parabola and the attracting center. It is clear that for such oscillations to be excited the light wave should be polarized parallel to the homogeneous field.

The electrons excited by a  $\sigma$ -polarized light wave have a nonzero angular momentum relative to the  $z$  axis and are emitted from the atom predominantly perpendicular to the  $z$  axis, so that the loops of their trajectories are not as densely spaced and they go off much

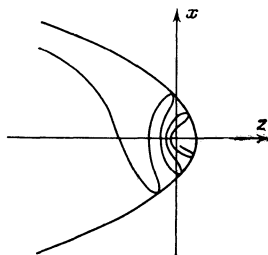


FIG. 3. Trajectory of motion of the electron after excitation when the light is polarized parallel to the uniform field.

more rapidly to infinity.

The condition  $Z_1(n_\xi) = 1$  has in terms of the initial variables the form of the quantization condition<sup>1)</sup>

$$\int_0^{\xi_1} \left( \frac{E}{2} + \frac{1}{\xi} - \frac{\mathcal{E}\xi}{4} \right)^{1/2} d\xi = \left[ n_\xi + \frac{1}{2}(m+1) \right] \pi, \quad (4.6)$$

at  $m=0$  this condition yields the function  $E(n_\xi)$  that determines the energy at which the partial cross section  $\sigma_{n_\xi, \text{of}}$  in the sum (2.6) reaches the maximum value. The maxima are reflected in the total cross section, and when the light is polarized parallel to the uniform electric field they cause oscillations in the region of low energies ( $E \ll 2\mathcal{E}^{1/2}$ ) in the dependence of the cross section on the energy. These oscillations were noted in an experimental investigation of the photoionization of rubidium atoms.<sup>7</sup>

Formula (4.6) can be made more precise by determining more accurately the value of  $Z_1^{(\text{max})}$  at the maximum of the cross section, by differentiating expression (3.24) for the corresponding partial cross section and separating the principal terms at  $E \ll 2\mathcal{E}^{1/2}$ . [The maxima in the dependences of the partial cross sections on  $Z_1$  and on the energy coincide, inasmuch as  $Z_1$  at fixed  $n_\xi$  is a monotonic function of the energy by virtue of (3.3)]. We determine the value of  $Z_1^{(\text{min})}$  at the minimum by considering in similar fashion the sum of two partial cross sections, for which  $Z_1$  is closest to  $Z_1^{(\text{max})}$ :

$$Z_1^{(\text{max min})} = 1 \mp \frac{k}{2\pi} \ln \frac{\pi}{2k}. \quad (4.7)$$

Thus, the equation ( $m=0$ )

$$\int_0^{\xi_1} \left[ \frac{k^2}{4} + \left( 1 \mp \frac{k}{2\pi} \ln \frac{\pi}{2k} \right) \frac{1}{\xi} - \frac{\mathcal{E}\xi}{4} \right]^{1/2} d\xi = \left( n_\xi + \frac{1}{2} \right) \pi \quad (4.8)$$

determines approximately the positions of the maxima (upper sign) and minima (lower sign) in the energy dependence of the cross section.

At sufficiently large  $n_\xi$ , Eqs. (4.6) and (4.8) lead to an approximately equidistant placement of the cross-section maxima. The distance  $\Delta E$  between the maxima near  $E=0$  is determined by the simple formula

$$\Delta E = \frac{dE}{dn_\xi} \Big|_{E=0} = 2\pi^{1/2} \frac{\Gamma(1/4)}{\Gamma(3/4)} \left( \frac{\mathcal{E}}{4} \right)^{1/4}. \quad (4.9)$$

This result was obtained in Ref. 9.

## 5. COMPARISON WITH EXPERIMENT

In the employed approximation, the dependence on the parameters of the initial and final states can be factored

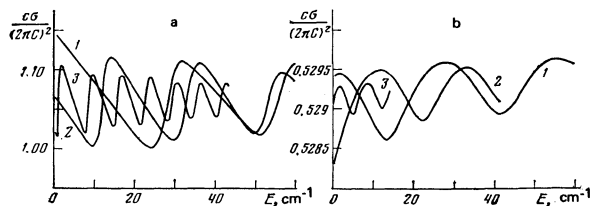


FIG. 4. Energy dependence of the relative photoionization cross section  $c\sigma/(2\pi C)^2$ , calculated for a uniform electric field intensity 6415 V/cm (1), 4335 V/cm (2), or 1016 V/cm (3) and for different polarization of the light wave (a— $m=0$ , b— $m=1$ ).

TABLE I. Position of the minima of the photoionization cross sections as functions of the energy at  $\mathcal{E} = 4335$  V/cm (in  $\text{cm}^{-1}$ ).

Experiment <sup>7</sup>	Calculation (2.6)	Calculation (4.8)	Experiment <sup>7</sup>	Calculation (2.6)	Calculation (4.8)
9.5±2	9.5	8.6	54±2	49.7	47.4
32±2	29.7	28.2	77±2	68.9	65.8

out in the cross sections (2.10) and (2.11). Therefore the relative cross section  $\sigma/C^2$  does not depend on the initial  $s$  state of the atom and is a universal function of the final-state energy  $E$  and of the constant-field intensity  $\mathcal{E}$ .

The photoionization cross section was calculated numerically by summing the partial cross sections in accordance with (2.6). The summation was confined to the values of  $m$  that are permissible for the given polarization in the final state and to the values of  $n_\ell$  at which  $\sigma_{n_\ell m \mathcal{E}}$  made a noticeable contribution to the cross section. The spectrum  $Z_1(n_\ell)$  was calculated in accordance with formulas (3.3)–(3.6), and expressions (3.21)–(3.24) were used to calculate  $\sigma_{n_\ell m \mathcal{E}}$ .

Figure 4 shows the results of the calculation of the dependence of the cross section on the energy for the cases for which experimental data are given in Ref. 7. We note first that the modulation of the cross section is smaller by two orders of magnitude at  $e \perp \mathcal{E}$  than at  $e \parallel \mathcal{E}$ . With increasing electric field intensity  $\mathcal{E}$  the amplitude of the oscillations, their period, and the energy region in which the oscillations are appreciable all increase.

Table I shows a comparison of the positions of the minima of the cross section with the experimental data for  $\mathcal{E} = 4335$  V/cm, shown in Fig. 3 of Ref. 7. Table II shows a comparison of the interval  $\Delta$  between the minima of the cross section in the vicinity of  $E = 0$  as a function of the intensity of the homogeneous field, with the experimental data shown in Fig. 4 of Ref. 7

To determine the positions of the maxima of the cross section in first-order approximation we can use Eq. (4.6). Table III gives a comparison of the positions of the maxima of the experimental curve of Fig. 1 of Ref. 7 with the values calculated from Eqs. (4.6) and (4.8) and with the maxima of the curves shown in Fig. 4. Account must be taken in the comparison of the finite energy resolution in the experiment, which shifts the

Table II. Interval  $\Delta$  between the cross-section minima closest to  $E = 0$  as a function of the intensity of the uniform electric field.

$\mathcal{E}$ , V/cm	$\Delta$ , $\text{cm}^{-1}$		
	Experiment <sup>7</sup>	Calculation (2.6)	Calculation (4.9)
1016	7.5±0.6	6.9	7.6
1600	11.3±0.7	9.7	10.7
2180	13.7±0.5	12.2	13.5
4335	22.7±0.5	20.2	22.6
6416	29.2±1	26.9	30.4
	31.5±1		

TABLE III. Positions of the maxima of the photoionization cross section as functions of the energy at  $\mathcal{E} = 4335$  V/cm (in  $\text{cm}^{-1}$ ).

Experiment <sup>7</sup>	Calculation (2.6)	Calculation (4.6)	Calculation (4.8)
17	14.1	11.8	15.9
39	36.2	33.1	38.8
–	56.5	53.3	59.9
–	75.8	72.5	79.8

maxima and minima on the experimental curve.

The depth of modulation of the calculated cross section ranges from 9 to 14% when the field intensity changes from 1016 to 6416 V/cm, whereas in the experiment the change ranges from 9 to 25%.

The oscillations of the type described in the present paper take place also at negative energies, but the resonances discussed in Sec. 1 are then superimposed on them in this region. The negative-energy region in which the damping of the oscillations takes place can be estimated by starting from the following considerations. For negative energies at  $Z_2 = 0$  the center of attraction turns out to be in the classically inaccessible region with respect to the parabolic coordinate  $\eta$ , owing to the presence of the uniform field. This leads to the appearance of a screening factor of the order of  $\exp(-|k|^3/3\mathcal{E})$  in the corresponding partial cross section, a factor corresponding to the uniform field in (2.3). The peak in the plot of  $\sigma_{n_\ell m \mathcal{E}}$  against  $Z_1$  becomes smoothed out at  $Z_1 \lesssim 1$ , and this leads to a damping of the considered oscillations at  $|k|^3/3\mathcal{E} \gtrsim 1$ , i.e.,  $E \lesssim -(3\mathcal{E})^{2/3}/2$ .

Thus, we can point out an energy interval in which the photoionization cross section is subject to oscillations due to the mentioned singularity of the classical infinite motion in the considered field:

$$-(3\mathcal{E})^{1/2}/2 \leq E \leq 2\mathcal{E}^{1/2}. \quad (5.1)$$

For  $\mathcal{E} = 4335$  V/cm we obtain therefore the inequality  $-20 \leq E \leq 400$   $\text{cm}^{-1}$ , i.e., at negative energies the cross section oscillates only once (cf. Table II).

The theory developed above connects the oscillations of the cross section with the singularities of the motion in a potential that admits of separation of the variables in parabolic coordinates. For a real multielectron atom, the single-electron potential at short distances differs from the Coulomb potential and an accurate separation is impossible. A characteristic of the short-range part of the potential can be the magnitude of the quantum defect, the empirical value of which for the rubidium atom is quite large (3.13), although it is close to an integer. Nonetheless, the theory describes well the experimental data for this atom. One can assume from general considerations that violation of the separability of the variables decreases primarily the depth of modulation of the cross section, but this is in fact not observed. A complete analysis of this prob-

lem, which is of interest to the physics of the Stark effect, can serve as the object of independent study.

<sup>1</sup>Formulas of this type, but different from (4, 6), were proposed without sufficient corroboration in Refs. 7 and 9.

<sup>1</sup>L. D. Landau and E. M. Lifshitz, *Kvantovaya Mekhanika* (Quantum Mechanics), Nauka (1974) [Pergamon].

<sup>2</sup>H. A. Bethe and E. E. Salpeter, *Quantum Mechanics of One- and Two-electron systems*, Springer, 1958.

<sup>3</sup>M. H. Rice and R. H. Good, *J. Opt. Soc. Am.* **52**, 239 (1962).

<sup>4</sup>R. Ya. Damburg and V. V. Kolosov, *Asimptoticheskiy podkhod k zadache Shtarka dlya atoma vodoroda* (Asymptotic Approach to the Stark Problem for the Hydrogen Atom), Zinatne, Riga, 1977; *J. Phys. B* **9**, 3149 (1976); **11**, 1921 (1978); **12**, 2637 (1979); *Opt. Commun.* **24**, 21 (1978).

<sup>5</sup>G. F. Drukarev, *Zh. Eksp. Teor. Fiz.* **75**, 473 (1978) [*Sov. Phys. JETP* **48**, 237 (1978)].

<sup>6</sup>S. Feneuille, S. Liberman, J. Pinard, and P. Jacquinet, *Compt. Rend. B238*, 291 (1977); S. Liberman and J. Pinard, *Phys. Rev. A* **20**, 507 (1979).

<sup>7</sup>R. R. Freeman, N. P. Economou, G. C. Bjorklund, and K. T. Lu, *Phys. Rev. Lett.* **41**, 1463 (1978).

<sup>8</sup>S. Feneuille and P. Jacquinet, *Proc. 6th Conf. on Atomic Physics*, 1978, p. 636.

<sup>9</sup>A. R. P. Rau, *J. Phys. B* **12**, L193 (1979).

<sup>10</sup>L. D. Landau and E. M. Lifshitz, *Mekhanika* (Mechanics), Nauka, 1973 [Pergamon].

<sup>11</sup>E. Clementi and C. Roetti, *Atomic Data and Nuclear Data Tables* **14**, Nos. 3-4, 1974.

<sup>12</sup>V. V. Beletskii, *Kosmicheskie issledovaniya* **2**, 408 (1964).

<sup>13</sup>V. V. Beletskii, *Proc. Conf. on Gen. and Appl. Problems of Celestial Mechanics*, Nauka, 1972, p. 213.

<sup>14</sup>V. V. Beletskii, *Ocherki o dvizhenii kosmicheskikh tel* (Studies of the Motion of Cosmic Bodies), Nauka, 1977.

Translated by J. G. Adashko

## Alignment of hydrogenlike atoms produced by electron capture in collisions of heavy charged particles with target atoms

E. G. Berezhko and N. M. Kabachnik

*Nuclear Physics Research Institute of the Moscow State University*

(Submitted 31 January 1980)

*Zh. Eksp. Teor. Fiz.* **79**, 409-421 (August 1980)

We investigate the alignment of excited states of hydrogenlike atoms produced by electron capture in collisions of heavy charged particles with target atoms. The degree of alignment, as well as the degree of polarization of the photons emitted upon decay of the excited states, is calculated in the Oppenheimer-Brinkman-Kramers approximation for a number of concrete cases. The dependence of these quantities on the velocity of the incident particle is investigated for various charge ratios of the particle and of the target-atom nucleus. The effect of cascade population of the excited state on the polarization of the radiation is investigated. The calculation results are compared with the available experimental data.

PACS numbers: 34.70. + e

1. This paper is devoted to a theoretical study of the alignment of the excited states of a single-electron  $B^{+(Z-1)}$ , which are produced as a result of capture of an electron when nuclei  $B^{+Z}$  collide with target atoms:

$$B^{+Z} + A \rightarrow B^{+(Z-1)*} + A^+ \quad (1)$$

The ion  $B^{+(Z-1)*}$  turns out to be in an aligned state because of the differences between the probabilities of populating the sublevels with different values of the projection  $|m|$  of the electron angular momentum on the direction of the incident beam. The degree of alignment of the excited state determines the polarization and the anisotropy of the angular distribution of the radiation produced in the successive transitions of the electrons to lower-lying states.<sup>1</sup>

The electron-capture cross sections in reactions (1) has recently been the subject of a tremendous number of theoretical as well as experimental studies (see, e.g., Ref. 2 and the literature therein), since these reactions play an important role in astrophysics, atmosphere physics, and plasma physics. Of particular interest, in connection with the problem of impurities in thermo-

nuclear plasma, are investigations of the capture into excited states.<sup>3</sup> Since the cross sections for capture into the excited states are determined in practice from the intensity of the radiation emitted at a definite angle as a result of the decay of these states, it is essential to know the angular distribution of this radiation. In addition, investigations of the excitation<sup>1</sup> and ionization<sup>4</sup> of atoms in collisions have shown that the study of the angular distribution and of the polarization of the radiation can yield additional information on the charge-exchange process itself, and is therefore of independent theoretical interest.

There are at present no published systematic data on the alignment of the excited states produced in the electron-capture process. Measurements of the degree of polarization of the  $L_\alpha$  emission of the hydrogen atom following capture of an electron by a proton in certain inert gases are reported in Refs. 5 and 6. These data, however, are not in agreement and are even contradictory. Measurement of the angular distribution of the characteristic  $x$  radiation produced when an elec-